

pubs.acs.org/estair Article

Sulfate and Carbonyl Sulfide Production in Aqueous Reactions of Hydroperoxymethyl Thioformate

Christopher M. Jernigan, Matthew J. Rivard, Max B. Berkelhammer, and Timothy H. Bertram*



Cite This: https://doi.org/10.1021/acsestair.3c00098



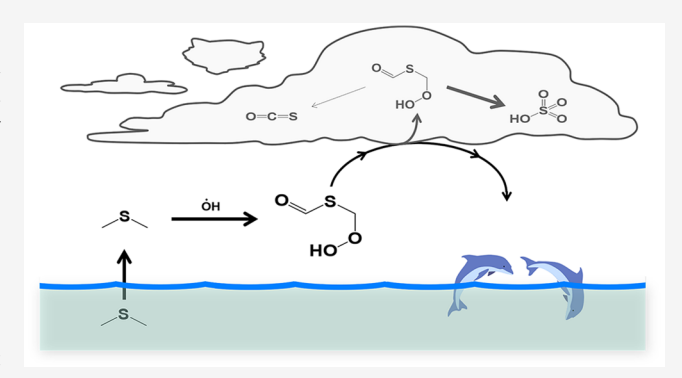
ACCESS

Metrics & More

Article Recommendations

Supporting Information

ABSTRACT: The oxidation products of dimethyl sulfide (DMS) contribute to the production and growth of cloud condensation nuclei (CCN) in the marine boundary layer. Laboratory and field measurements have demonstrated that DMS is oxidized by hydroxyl radicals (OH) forming the stable intermediate hydroperoxymethyl thioformate (HPMTF) in high yield. HPMTF is both globally ubiquitous and efficiently lost to multiphase processes in the marine atmosphere. At present, there are no experimental measurements of the products of aqueous reactions of HPMTF. Prior modeling studies have assumed that HPMTF is irreversibly lost to aqueous interfaces arresting carbonyl sulfide (OCS) and sulfur dioxide (SO₂) production and forming sulfate at unit yield. Here, we use a custom-built bubbler apparatus



combined with chemical ionization mass spectrometry (CIMS) for detection of gas-phase HPMTF, a commercial quantum cascade laser system for detection of OCS, and ion chromatography for measurement of condensed phase products. We show that the molar yield of OCS and sulfate (SO_4^{2-}) from the hydrolysis of HPMTF is <1.2% and 122 \pm 46%, respectively. The results suggest that sulfate is formed in near unit yield in the cloud processing of HPMTF, and we discuss both the chemical mechanism for sulfate formation and potential for reactive solutes to alter this reaction mechanism.

KEYWORDS: Dimethyl sulfide, aqueous processing, marine, laboratory observation, hydroperoxymethyl thioformate, sulfate, carbonyl sulfide

1. INTRODUCTION

Dimethyl sulfide (DMS) is produced and emitted from the ocean leading to a significant source of reduced sulfur to the atmosphere. 1,2 Once emitted, DMS is oxidized by either the hydroxyl radical (OH) or halogen radicals (e.g. BrO, Cl) resulting in the formation of low volatility oxidation products that can nucleate new or grow existing aerosol particles to cloud condensation nuclei (CCN) sizes. 3-6 Until recently, the oxidation mechanism for DMS in the majority of chemical transport models was largely simplified to only include sulfur dioxide (SO₂) and methanesulfonic acid (MSA) as the stable products of DMS oxidation, where the branching between their production rates is a function of temperature. ⁷⁻⁹ SO₂ can be further oxidized to sulfuric acid (H₂SO₄) leading to new particle formation, while MSA contributes to particle growth through condensation.¹⁰ Recent computational, laboratory, and field work has demonstrated that the OH-oxidation of DMS leads to the efficient production of hydroperoxymethyl thioformate (HPMTF; HOOCH₂SCHO), a stable, soluble reaction intermediate.11-14 The gas-phase reaction of HPMTF with OH has a rate constant $(k_{HPMTF+OH})$ of 1.4×10^{-11} cm³ molec⁻¹ s⁻¹ at 298 K, leading to an average gas-phase lifetime of 20 h ([OH] = 1.0×10^6 molec·cm⁻³).¹⁵ The reactive uptake of HPMTF to marine aerosol particles depends on particle phase and chemical composition. The reactive uptake coefficient of HPMTF ($\gamma_{\rm HPMTF}$) to deliquesced NaCl particles has been measured to be 1.6×10^{-3} , leading to a lifetime of 53 h for particle surface area concentrations of 50 $\mu{\rm m}^2$ cm⁻³.¹¹ Further, HPMTF has been shown to be efficiently lost to marine clouds which is the dominant loss process in the cloudy marine boundary layer.^{9,11,12,15,16} It has been suggested that condensed phase chemistry of HPMTF is irreversible, arresting the formation of SO₂ and OCS that are efficiently produced in the gas-phase OH-oxidation of HPMTF.^{9,11,15,16}

Here, we present laboratory measurements of the OCS and sulfate yield from the hydrolysis of HPMTF in water using a custom-built bubbler combined with gas and aqueous phase sulfur measurements. Observations of the OCS and sulfate product yields at near neutral pH and in the absence of solutes

Received: December 1, 2023 Revised: April 2, 2024 Accepted: April 3, 2024



are used to infer the hydrolysis mechanism that is likely to dominate in reactions occurring in dilute cloud droplets.

2. METHODS AND MATERIALS

2.1. Generation and Detection of Hydroperoxymethyl Thioformate. In the absence of a pure source of HPMTF available for experimentation, HPMTF ([HPMTF] = 800-1200 ppt) was generated from the NO₃-initiated oxidation of DMS in a 0.6 m³ PTFE environmental chamber. The environmental chamber was operated in a continuous flow mode at ambient temperature (298 K) and 1 atm of dry (<80 ppm of H₂O) zero air, as described in Jernigan et al. (2022). Previous experimentation on HPMTF used the dark ozonolysis of tetramethyl ethene (TME) to generate the hydroxyl radical (OH) and initialize the oxidation of DMS and formation of HPMTF. Here, we oxidize DMS with nitrate radicals (NO₃) as HPMTF is formed in near unit yield in the NO₃ + DMS reaction and the relatively slow reaction of NO₃ with HPMTF.

DMS and NO₂ were supplied to the chamber from compressed gas cylinders (Praxair, dimethyl sulfide at 5.08 ppm in N₂ and Airgas, nitrogen dioxide at 1.19 ppm in N₂), resulting in an initial DMS and NO₂ concentration of 8.7 and 4.7 ppb in the chamber. Ozone (O₃), used for initializing the formation of NO₃, was supplied to the chamber by a custombuilt ozone generator previously described in Jernigan et al. (2022) resulting in 60–80 ppb of O₃ in the chamber. To ensure all species within the chamber outflow reached a stable concentration, the chamber was run for >20 h before the aqueous HPMTF experiments were started. Under the conditions described above ([DMS]_I = 8.7 ppb, [NO₂]_i = 4.7 ppb, and [O₃]_i = 60 ppb), a steady-state concentration of HPMTF of 800–1200 ppt was observed.

HPMTF, nitric acid (HNO₃), nitrogen dioxide (NO₂), and SO₂ were quantified with a Aerodyne/TofWerk Compact Time of Flight (C-ToF) Chemical Ionization Mass Spectrometer utilizing iodine and oxygen anion chemistry. ^{15,17-19} Carbonyl sulfide (OCS) and water vapor (H₂O) measurements were made using a Los Gatos Research, Enhanced Performance OCS analyzer (PN:914-0028), previously described by Berkelhammer et al. (2014). ²⁰

Under dark conditions, NO₃ can react further with NO₂ forming dinitrogen pentoxide (N2O5) which establishes a thermal equilibrium with NO₃. N₂O₅ is detected as a cluster with iodide ($[I\cdot N_2O_5]^-$) at 235 m/Q which is isobaric with HPMTF given the resolving power of the ToF mass analyzer used in this study (m/ Δ m = 800). To minimize N₂O₅ production, we run the chamber in excess O₃ which suppresses NO₂ concentrations and N₂O₅ production. To definitively determine whether N2O5 was forming in the chamber and contributing to the detection of HPMTF, we conducted an experiment using a compressed cylinder containing 1.14 ppm of dimethyl-1,1,1-d₃ sulfide (DMS-D₃) in nitrogen. By utilizing DMS-D₃, the deuterated HPMTF product is detected as $H_2D_2C_2SO_3$ at 237 m/Q₄ 2 mass units from the peak associated with N_2O_5 . In these experiments, no signal was detected at 235 m/Q confirming that N₂O₅ does not contribute to HPMTF detection in our experiment. All subsequent aqueous HPMTF experiments discussed here were performed with nondeuterated DMS.

2.2. Determination of Carbonyl Sulfide and Sulfate Formation from Aqueous Reactions. The carbonyl sulfide and sulfate yield from HPMTF hydrolysis was determined using a custom-built fritted bubbler system (Figure 1). The fritted

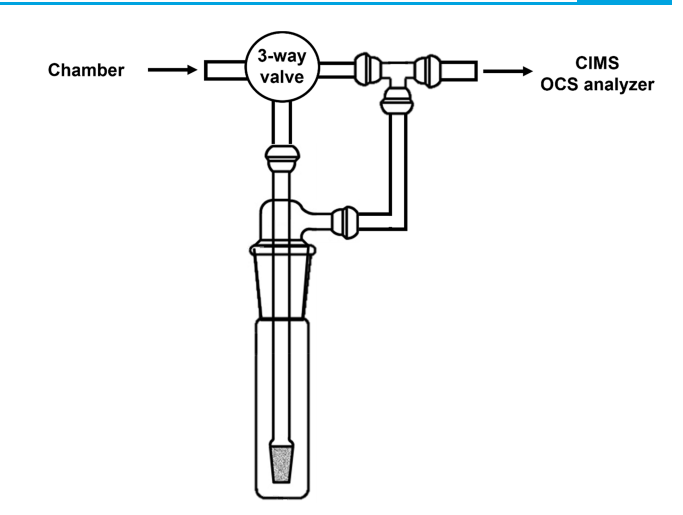


Figure 1. Schematic of the HPMTF bubbler system.

bubbler system was made from a coarse grain glass fritted set within a glass receptacle. The use of a glass fritted system provides a potentially reactive surface not present in an ambient cloud or aerosol, but irreversible loss of HPMTF was found when a 1/16" ID PFA tube was used instead of glass. The effluent of the environmental chamber is connected to a PTFE three-way solenoid valve to direct flow either through the bubbler or a bypass line prior to detection with the gas-phase instruments. Each experiment was run by passing 650-700 standard cubic centimeters per minute (sccm) of chamber air through the glass receptacle containing 20 mL of ultrapure Milli-Q water (Milli-Q Reference). A consistent flow from the chamber was supplied to the bubbler with a microdiaphragm gas pump (UNMP 830 Series). For each experiment, the chamber air was pulled from the chamber through the diaphragm pump to the instrumentation via the glass fritted system or a bypass line. The pump flow used for calculation of the production yield was measured between experiments using an inline flow meter (TSI Model 4043). All experiments were run by overflowing the instruments to eliminate the potential of sampling ambient air.

We calculate the OCS product yield (Φ_{OCS}) from the hydrolysis of HPMTF as the ratio of the change in the OCS signal ($\Delta_{OCS} = [OCS]_{bubbler} - [OCS]_{bypass}$) to the change in the HPMTF signal ($\Delta_{HPMTF} = [HPMTF]_{bypass} - [HPMTF]_{bubbler}$). To determine Φ_{OCS} , we vary the HPMTF concentration (and thus Δ_{HPMTF}) by diluting the chamber air outflow with liquid nitrogen boil off and measure the response in Δ_{OCS} . To account for the known dependence of the measured OCS concentration on the gas-phase water concentration as measured by the OCS analyzer, water sensitivity tests were performed across the observed water and oxidant concentrations.

To determine the sulfate product yield (Φ_{SO4}) , an ion chromatography (IC) system was used to measure the concentration of sulfate in the bubbler water. In this experiment, Δ_{SO4} is determined from the measured $SO_4^{\ 2^-}$ in the blank and bubbler water. To determine Φ_{SO4} , we varied Δ_{HPMTF} by changing the duration of time that chamber air is flowed through the bubbler.

After each bubbling experiment, 2 mL of water was extracted from the bubbler apparatus and stored in a 2.5 mL plastic IC vial under refrigeration until ICs could be performed. The remaining volume within the bubbler system was measured to determine the amount of $\rm H_2O$ evaporated during the experiment. A water volume of 20 mL was used to ensure the bubbler system was

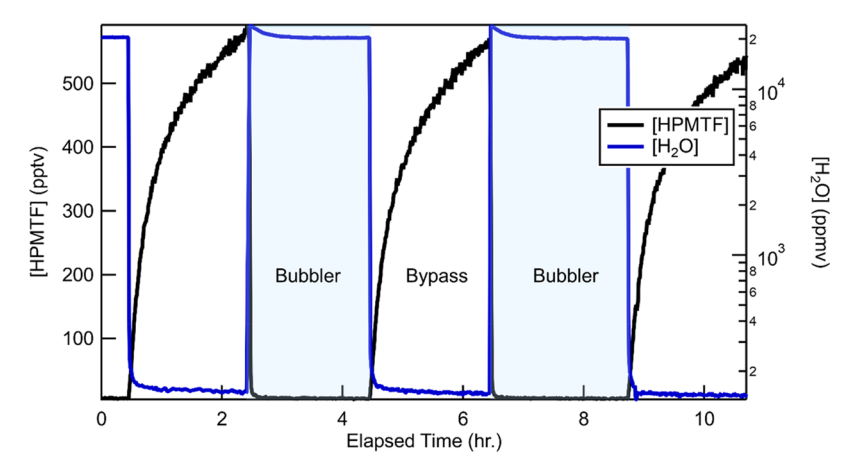


Figure 2. HPMTF (black trace) and water (blue trace) measured at the end of the bubbler system during a representative experiment where chamber air is modulated through (blue section) and bypasses (white section) the bubbler system.

completely submerged throughout the entire experiment. We measure a consistent 0.8 mL h^{-1} loss in water when 680 sccm of dry air is flowed through the bubbler system.

The sulfate concentration was determined by ion chromatography (IC), conducted on a Thermo Electron Dionex chromatography system. An AS-18 250 mm analytical column and a 50 mm guard column were used, both 2 mm in diameter, with a 23 nM solution of KOH used as the eluent. The system was run under a constant current and flow rate at 15 A and 0.250 mL min $^{-1}$ for 15 min, respectively. The IC system was calibrated for sulfate with varying sulfate concentrations prepared via a gravimetric technique. A stock solution of about 80 ppm of SO_4^{2-} was generated from dissolved magnesium sulfate (Sigma-Aldrich, >97.0% purity), and serial dilutions were undergone to obtain solutions of known sulfate concentration between 1 and 50 ppb (See SI, Figure S1).

It is well established that sulfate is also produced in the aqueous reaction of SO_2 and O_3 , both of which are present in the environmental chamber effluent ($[SO_2] < 1$ ppb and $[O_3] = 75$ ppb). To account for sulfate formed from this reaction, we also conducted an experiment where we mix SO_2 and O_3 , at concentrations equal to that of the chamber effluent (0.86 and 75 ppb, respectively), and determine the corresponding sulfate production rates. This correction factor is discussed in detail in section 3.3.

3. RESULTS AND DISCUSSION

3.1. Production of HPMTF in the NO₃ Oxidation of **DMS.** The chemical mechanism and kinetics of HPMTF formation from the NO₃ oxidation of DMS will be addressed in detail in a forthcoming manuscript. Here, we briefly describe the chemistry of HPMTF production from the reaction of DMS with NO₃ as it relates to this experiment. The nitrate radical (NO_3) is generated via the reaction of NO_2 with O_3 . The environmental chamber was run in excess O_3 ($[O_3]_i = 60-80$ ppb) as compared to NO_2 ([NO_2]_i = 3-5 ppb), leading to the efficient formation of NO_3 ($O_3 + NO_2 \rightarrow NO_3$) while limiting the production of N_2O_5 ($NO_3 + NO_2 = N_2O_5$). These conditions also lead to the efficient conversion of nitric oxide (NO) to NO₂ within the chamber (NO + O₃ \rightarrow NO₂ + O₂) and eliminate photolytic reactions leading to the regeneration of NO from NO₂ (NO₂ $\stackrel{h\nu}{\rightarrow}$ NO + O(³P)). The result of the environmental oxidative conditions is a sustained near zero concentration of NO, which eliminates the bimolecular reaction

of NO with organic peroxy radicals (RO₂·) that competes with the intramolecular chemistry that leads to HPMTF formation. NO₃ has the potential to react competitively with the proxy radical that precedes HPMTF, methylthiomethylperoxy radical (MTMP; CH₃SCH₂O₂•). The low chamber concentrations of NO₃, the direct formation of MTMP from DMS + NO₃, and the assumed slow reaction of NO₃ with MTMP ($k_{MTMP+NO3} = 2.3 \times$ 10^{-12} cm³ molec⁻¹ s⁻¹, taken from CH₃CH₂O₂ \bullet + NO₃) lead to a chemical regime where NO3 oxidation yields HPMTF from DMS in near unit yield.²² In addition, we expect the reaction of NO₃ with HPMTF to be slower than OH + HPMTF, based upon the assumption that HPMTF will react with NO₃ at rates similar to sulfur containing and aldehyde containing compounds $(1-3 \times 10^{-13} \text{ cm}^3 \text{ molec}^{-1} \text{ s}^{-1})$. The assumed slow oxidative loss process would result in the longer chamber lifetime and higher steady-state concentration observed.

The decision to generate HPMTF from DMS + NO₃ rather than DMS + OH was to reduce the production of OH-addition products within the DMS oxidation mechanism and the production rate of SO₂ from HPMTF + OH, all of which may contribute to sulfate formation in the experiment. 15 The products of the OH-addition channel include dimethyl sulfoxide (DMSO), methane sulfinic acid (MSIA), and methanesulfonic acid (MSA) each of which can oxidize to sulfate in the condensed phase.²⁴ Based on both CIMS observations and model outputs, HPMTF, DMS, and SO2 are the dominate sulfur-containing molecules in the NO3 oxidation chamber effluent. Trace amounts of DMSO, MSIA, and MSA were observed in the chamber experiments (<50 ppt) and were assumed to form through the OH oxidation of DMS. Our modelling results suggest that the isomerization of MTMP, where OH is generated, accounts for > 85% of the OH produced ([OH] $_{SS, model}$ = 0.05 ppt). While these species are detectable in the chamber, they are scavenged by the diaphragm pump used to direct chamber air to the bubbler system. A significant loss of HPMTF (31 \pm 11%) was also observed in the pump system, which is accounted for in our experimental determinations of $\Phi_{\rm OCS}$ and $\Phi_{\rm SO4}$. The concentration of HPMTF, SO₂, and O₃ used for analysis was calculated from the output of the pump and was measured before each experiment. The contribution to sulfate from the oxidation of aqueous DMS by either OH or ozone is expected to be minimally compared to SO₂ oxidation due to the lack of OH production (e.g. via photolysis or Fenton) and the DMS oxidation mechanism in the bubbler. 25 While both

DMS and SO_2 have relatively fast reaction rates with ozone at a neutral pH ($10^8 \, M^{-1} \, s^{-1}$), only SO_2 oxidation efficiently yields sulfate. ^{26,27} The primary product of DMS + O_3 is DMSO, whose slow reaction rate with O_3 (4.3 $M^{-1} \, s^{-1}$) arrests the potential for dissolved DMS driven sulfate production on the time scale of the presented experiments. ^{26,27} Production of sulfate from SO_2 , and its impact on the determination of Φ_{SO4} , is discussed in detail in section 3.3.

To evaluate the dependence of sulfate production on sample age (time between sample collection and analysis), vials of similar chamber exposure but differing time between collection and IC analysis were compared. No statistical differences in sulfate were found for sample storage times up to 6 days. The absence of any measured time dependence in sulfate production suggests that condensed phase sulfate formation that proceeds through slower intermediate-driven mechanisms (e.g. DMSO oxidation) or leaching of sulfate from the vials was not important in this experiment.

3.2. Aqueous Production of Carbonyl Sulfide from **DMS Oxidation.** A typical OCS production experiment is shown in Figure 2, where HPMTF is directed either through the bypass or the bubbler assembly and detected by CIMS. HPMTF is efficiently and irreversibly lost upon routing the chamber air flow through the water bubbler. The HPMTF signal during the bubbling phase remains at concentrations below the CIMS detection limit for sampling periods as long as 8 h, indicating that HPMTF does not accumulate or equilibrate in the water reservoir but is efficiently and irreversibly lost to hydrolysis (See SI, Figure S2). This result is consistent with laboratory and field observations of HPMTF that show it to be irreversibly lost to aerosol particles and clouds. 11-13,16 A significant recovery time in the HPMTF signal is observed when switching between the bubbler and bypass lines. The extended rise time is assumed to be associated with the drying of the walls throughout the tubing and within the IMR of the CIMS instrument. We assume that all HPMTF is lost to the water in the bubbler and that the subsequent tubing does not contribute to additional HPMTF loss. As such, the reference concentration of HPMTF is determined from the steady state concentration of HPMTF in the bypass flow.

The difference in the water vapor mixing ratio between the bypass and bubbler lines is substantial ($[H_2O]_{bypass} > 80 \text{ ppm}$ and $[H_2O]_{bubbler} = 2.0 \times 10^4 \text{ ppm}$). This change in absolute humidity presents challenges for the on-line gas-phase instrumentation that needs to be accounted for. ^{28–30} In the case of the CIMS measurements of HPMTF, the [HPMTF] in the bubbler air was always below the method detection limit. As a result, the HPMTF sensitivity determined for dry air was applied to retrieve HPMTF concentrations. 12,13 To account for the humidity induced background change in the OCS measurement, an empirical humidity correction was applied to the OCS measurements. To determine the experimental production of OCS without sulfur present, chamber air containing the same oxidative conditions (i.e. $NO_2 + O_3 \rightarrow$ NO₃) without DMS present was routed through and bypasses the bubbler. The average baselines of OCS under the dry and wet conditions were used to determine the background intensities of OCS. Lastly, natural fluctuations associated with instrument drift overtime were normalized to remove variations in the OCS concentrations not associated with HPMTF bubbling. As seen in Figure 3, no detectable change in OCS was observed during the HPMTF bubbling experiments, where $\Delta_{\rm HPMTF}$ = 690 \pm 140 ppt. Using a 300-s averaging time, the

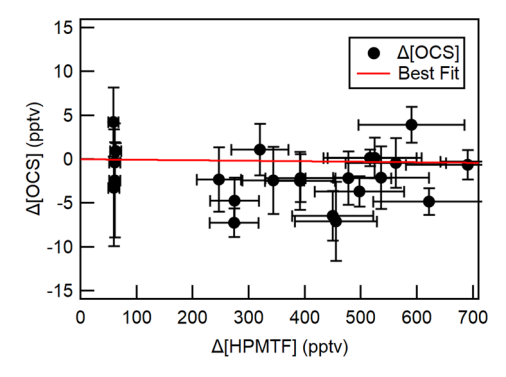
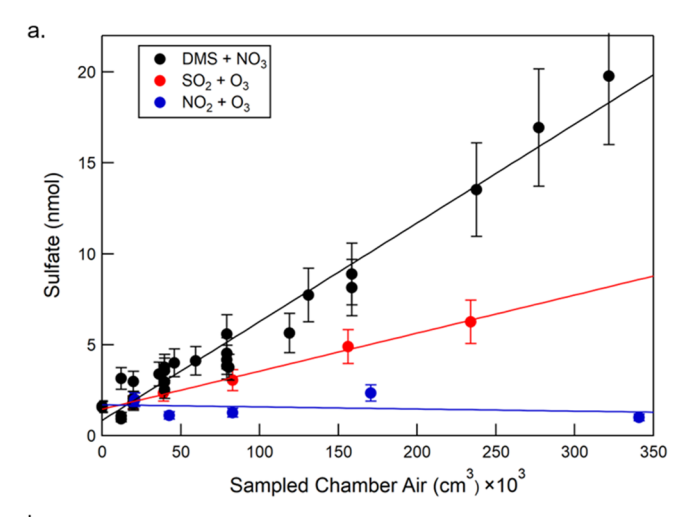


Figure 3. Concentration of carbonyl sulfide (black dots) as a function of HPMTF lost to the bubbler apparatus. The best fit through the experimental observations is presented as the red trace with a slope < 0.001.

smallest OCS concentration observable for the baseline concentrations measured here is 7 ppt. If we take this as the minimum observable Δ_{OCS} , we calculate an upper limit for the OCS yield from HPMTF hydrolysis (Φ_{OCS}) of 1.2%.

The OCS yield presented here does not consider the potential for OCS to hydrolyze, form organic acids, decompose to sulfides, and reduce the observed OCS yield from HPMTF hydrolysis.³¹ The lifetime of OCS is orders of magnitude longer than the primary hydrolysis product (monothiocarbonic acid, MTC) at neutral pH, which would favor OCS formation and emission over dissolution in the bubbler. Under atmospheric conditions where photolysis, varying pH, and less ozone is present, HPMTF and its hydrolysis products could react in different mechanisms forming OCS. Future work should be focused on determining the condensed phase mechanism that connects HPMTF to OCS.

3.3. Aqueous Production of Sulfate (SO_4^{2-}) from DMS Oxidation. The sulfate molar yield from HPMTF hydrolysis was determined as the ratio of the moles of HPMTF derived sulfate produced to the moles of HPMTF lost to solution. We experimentally determine non-HPMTF derived sulfate, generated in the $O_3 + SO_2$ reaction and residual sulfate present in glassware, by conducting an experiment where chamber air containing NO₂, O₃, and SO₂ (at concentrations comparable to that observed in the experiment) was run through the bubbler system. SO₂, O₃, and NO₂ concentrations exiting the pump were measured using the CIMS, operating in oxygen anion mode, where SO₂ is detected as SO₂⁻ at 64 m/Q, O₃ is detected as CO_3^- at 60 m/Q, and NO_2 is detected as NO_2^- at 46 m/Q. ¹⁸ The production of sulfate in each of these experiments is presented in Figure 4a as a function of the volume of air sampled through the bubbler. Water evaporation from the bubbler system during the experiment (0.8 mL h^{-1}) was accounted for in the calculation of the molar yield of sulfate. Vigorous bubbling allowed for small bubbles and high surface area exposure of the chamber air, as well as an increase in agitation and bubble bursting promoting potential gas (e.g. OCS) emission. In Figure 4a, the x-axis is sampled chamber air volume to account for the collection of sulfur species, some of which can oxidize to sulfate (e.g. SO₂, HPMTF), that are present in the chamber outflow. The oxidized chamber air without DMS present showed little to no production of sulfate (<0.2 nmol $SO_4^{2-} h^{-1}$) illustrating the lack of sulfate production from the apparatus and sample preparation (e.g. leaching from glass) (Blue line, Figure 4a). The contribution to sulfate from the reaction of SO_2 and O_3 was determined by subtracting the sulfate yield from the best fit of



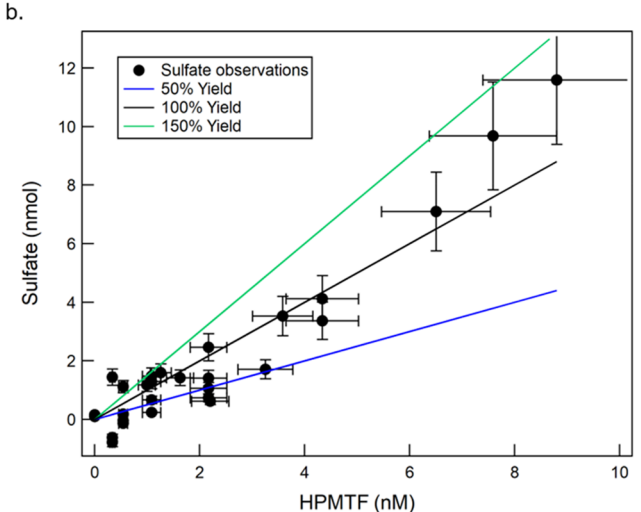


Figure 4. (a) The moles of sulfate $(SO_4^{\ 2-})$ calculated by IC that was found by bubbling a set volume of chamber air through a custom bubbler apparatus. Air containing the reactants and products of a DMS + NO₃ chamber with DMS present (black dots), background reactants from a chamber exposed to NO_3 (generated from $NO_2 + O_3$) without DMS present (blue dots), and air containing ozone (O₃) and sulfur dioxide (SO₂) at the similar concentrations of the DMS + NO₃ chamber with DMS present experiment (red dots) are shown. A linear fit is drawn through each of the three experiments to indicate the relative slope of each. The linear least square R² value of DMS + NO₃, $SO_2 + O_3$, and $NO_2 + O_3$ is 0.964, 0.995, and 0.066, respectively. (b) The moles of sulfur in the form of sulfate taken from the difference in sulfate mass from the DMS + NO₃ chamber with DMS present experiments between that of an exposure weighted sulfate mole if only SO₂ and ozone were present regressed against the moles of sulfur in the form of HPMTF that was taken up by the bubbler solution is shown (black dots). A percent yield of 50 (blue trace), 100 (black trace), and 150 (green trace) from the HPMTF to form sulfate is shown.

the $SO_2 + O_3$ analysis at various volumes of chamber air (**Red line**, Figure 4a). A significant amount of sulfate was produced when SO_2 and O_3 (at concentrations representative of that in the HPMTF experiment) were sampled through the bubbler. For initial O_3 and SO_2 concentrations of 75 and 0.86 ppb, respectively, we determine a molar yield of 0.55–0.65 for the fraction of SO_2 that passed through the bubbler system that was converted to sulfate (See SI, Figure S3). Sulfate production from all sulfur containing gases present in the full experiment is shown with the black line in Figure 4a. To determine the sulfate yield

from HPMTF, we subtract the sulfate formed from the SO_2+O_3 reaction (red line) from the sulfate formed in the combined experiment (black line). The amount of HPMTF (units of nanomoles of HPMTF) lost to water was calculated from the mixing ratio of HPMTF in the chamber outflow that passes through the bubbler (670 \pm 110 pptv; 1.65 \times 10 10 molec/cm³), the flow through the bubbler (sccm), and the amount of time bubbling (minutes). As shown in Figure 4b, the slope of the best fit line returns a sulfate molar yield from HPMTF hydrolysis of 1.22 \pm 0.46. The uncertainty in the determination is driven primarily by uncertainty in the sensitivity of HPMTF and the contribution of SO_2+O_3 to sulfate formation.

While a sulfate product yield greater than 100% from HPMTF is within the total uncertainty of the experiment, there are several additional sulfate formation channels and/or experimental factors that may contribute to excess sulfate formation. These include:

- 1) The reaction of the hydroperoxide (ROOH) functional group in HPMTF (or other peroxides present in the environmental chamber) with dissolved S(IV) to form sulfate. 32,33 The presence of the ROOH functional group could enhance the formation of sulfate by increasing the routes of oxidation of available S(IV), in particular SO₂ from the chamber. The contribution of sulfate from the hydrolysis and ozone of oxidation of SO₂ is accounted for in the control experiment (Red line, Figure 4a), but additional oxidation could occur facilitated by ROOH present in the DMS + NO₃ chamber air. A benefit of generating HMPTF through NO₃· + DMS chemistry is a reduction in total gaseous ROOH (generated from the oxidation of TME) that is formed through previous methods of HPMTF generation. 15 The environmental chamber is set up to promote RO2 chemistry and isomerization reactions, but a minor production of HO₂ still exists as validated by the observation of a ROOH species originating from an TME RO2 species.
- 2) The oxidation of S(IV) present in the Milli-Q water by NO₂ could lead to enhanced sulfate formation.³⁴ The control experiment targeting SO₂ + O₃ did not contain NO₂, as the target was to determine the yield from only SO₂ and ozone. Additionally, the output of the chamber did not provide a detectable signal of NO₂ (detected as [NO₂][−] in the oxygen anion CIMS instrument) above the baseline. The low concentration of NO₂ is controlled by the elevated concentration of ozone and dark conditions within the chamber which can titrate NO₂ (via NO₂ + O₃ → NO₃) and arrests NO₂ production from NO₃ photolysis, respectively. Without detectable concentrations of NO₂ present in the chamber air sampled through the bubbler, the enhanced sulfate yield is not thought to be enhanced by an NO₂ pathway.
- 3) As shown in Figure 4b, deviation from the 100% yield line arises at larger chamber exposures and bubbling time. The vigorous bubbling leads to significant losses (up to 35%) in water over the course of multiple hours which could lead to chamber air sampled at later times (>8 h) experiencing and contributing to elevated concentrations of aqueous species, potentially increasing the rate of reactions leading to sulfate. Sulfate samples used for the calculation of the molar yield were normalized to the initial volume of water (20 ml) in the bubbler to account for deviations in sulfate as a function of evaporation, while

Figure 5. Potential oxidative mechanisms driving HPMTF oxidation to sulfate.

the sulfate concentrations were quantified using an aliquot of the bubbled solution. Additionally, the samples demonstrating nonlinearity were also outside the range of the $SO_2 + O_3$ control experiments as well as the IC sulfate calibrations. We hypothesize that the reduced volume of water in the bubbler could lead to an effective increase in concertation of dissolved sulfur and ozone, adding to an increase in the production rate of sulfate not captured in the control experiments. If experimental points that sampled large volumes and times of chamber air (>2.50 × 10^5 cm³ or 8 h) and lay outside the IC sulfate calibration range $(0-50 \text{ ppb } SO_4^{2-})$ were removed from the analysis, a molar yield of $96 \pm 35\%$ was found for the aqueous conversion of HPMTF to sulfate.

4. CONCLUSIONS AND ATMOSPHERIC IMPLICATIONS

We report measurements of product yields of OCS and sulfate from the condensed phase hydrolysis of HPMTF. We determine an OCS product yield from HPMTF hydrolysis of <1.2% and a molar sulfate yield of 122 \pm 46%. These measurements confirm the original hypothesis that HPMTF is irreversibly lost in cloud water with a near unit product yield of sulfate.

While these experiments did not permit a direct assessment of the HPMTF hydrolysis and oxidation reaction mechanism, a proposed mechanism consistent with the high yield of sulfate and presence of ozone is proposed based on the molecular structure of HPMTF. We suspect that HPMTF undergoes a hydrolysis reaction similar to other carbonyl species, which starts with the hydrogenation of the carbonyl group (Figure 5). Previous studies have shown that this pathway, typically catalyzed by the presence of an acidic aerosol, is the dominant pathway for carbonyl loss. The support for potential HPMTF reactions in the aqueous medium can be drawn from known chemistry of hydroperoxmethyl formate (HPMF), a structurally similar molecule produced from dimethyl ether oxidation, and the oxygen analogue to HPMTF is replaced by an oxygen. Thamm et al. (1996) found HPMF to have an

aqueous lifetime of 7 and 140 min at pH's of 3.5 and 1.0, respectively. HPMF was found to be stable when dissolved in chloroform and reacted rapidly in aqueous solutions, unless the solution was strongly acidic.

Alternatively, HPMTF could undergo a 1,5 cyclization and decomposition in water, similar to that of cyclic peroxyhemiacetals. The postulated pathway forms a cyclic hydroperoxyl aldehyde that could later decompose into a set of sulfur containing organic acids. Whether HPMTF is lost through a carbonyl loss pathway or through the cyclization/decomposition, the products of either of these reactions could result in the production of more water-soluble organic acids. ³¹

The fate and reaction mechanisms of the various sulfurcontaining organic acids and thiols proposed in Figure 5 could not be directly observed within the following experimental design. The high yield of sulfate and presence of ozone within the outflow of the chamber would favor oxidative reactions initialized by ozone, rather than hydroxy $(\bullet OH)$ and hydrogen peroxide (H2O2), both of which typically are required by photolysis or transition metals to be produced in substantial yields. ^{25,43,44} We propose the primary route of sulfate formation in our system would be through the reactions of ozone with any of the various thiols (RSH) and thioacids (RC(=O)SH) potentially formed in the bubbler. Under the neutral conditions within the bubbler, the proposed thioacids formed would preferentially deprotonate as thioacids are typically more acidic and nucleophilic than their carboxylic analogues.⁴⁵ The thiolate (RS⁻) form of the sulfur species would both increase the potential for them to remain in the aqueous phase under rigorous bubbling and increase the rate of reaction with ozone. 46-48 The oxidation of thiol/thiolates is fast and thought to transit through sulfenic (RSOH), sulfinic (RS(=O)OH), and sulfonic (RS(=O)₂OH) acid. ^{48,49} As available literature on the ozone oxidation of the proposed thioacids and functionalized thiols could not be found, we proposed mechanisms based on hydrogen sulfide (H₂S), methanethiol (CH₃SH), and hydroxymethanesulfonate (HMS, HOCH₂SO₃H). We propose each available R-SH will eventually oxidize to form sulfinic or sulfonic acids. The increased functionalization, including

hydroxyl (-OH), hydroperoxyl (-OOH), or formyl (-CHO) groups, of the proposed acids could increase the potential for the formation of sulfate through historic reactions involving aldehydes and bisulfite (HSO_3^-). So -52 Using these mechanisms as guidance, we propose that the various sulfur compounds precede primarily through HPMTF hydrolysis and subsequently through ozone oxidation to sulfate.

The high yield of sulfate, assumed oxidation through thiols, and lack of OCS observed from the bubbling experimentation would imply that the sulfur species formed here are preferentially going on to form sulfate rather than through decomposition to OCS. The results presented here support the current understanding that the loss of HPMTF to aerosol and cloud surfaces is irreversible, and aerosol and cloud loss of HPMTF leads to a decrease in the global SO₂ and OCS production. The work performed here can be utilized to better understand the impact of DMS emission on sulfate aerosol production. Future work should be focused on determining the condensed phase mechanism that connects HPMTF to sulfate. In particular, a focus on the role of ionic strength and acidity should be considered as they are critical components of atmospheric surfaces.

ASSOCIATED CONTENT

Supporting Information

The Supporting Information is available free of charge at https://pubs.acs.org/doi/10.1021/acsestair.3c00098.

A description of the 0D Box model and inputs for DMS + NO_3 and the calibration of the CIMS and OCS instruments, Supporting figures relating to the IC calibrations, 8-hour HPMTF bubbling experiment, and fraction of observed sulfate from aqueous $SO_2 + O_3$ (PDF)

AUTHOR INFORMATION

Corresponding Author

Timothy H. Bertram — Department of Chemistry, University of Wisconsin, Madison, Wisconsin 53706, United States; orcid.org/0000-0002-3026-7588; Phone: 608-890-3422; Email: timothy.bertram@wisc.edu

Authors

Christopher M. Jernigan — Department of Chemistry, University of Wisconsin, Madison, Wisconsin 53706, United States; Present Address: Cooperative Institute for Research in Environmental Sciences (CIRES), University of Colorado-Boulder, Boulder, CO 80309, USA; Present Address: National Oceanic and Atmospheric Administration (NOAA) Chemical Sciences Laboratory (CSL), Boulder, CO 80305, USA.; orcid.org/0000-0003-0302-5222

Matthew J. Rivard — Department of Chemistry, University of Wisconsin, Madison, Wisconsin 53706, United States

Max B. Berkelhammer — Department of Earth and
Environmental Sciences, University of Illinois Chicago,
Chicago, Illinois 60607, United States

Complete contact information is available at: https://pubs.acs.org/10.1021/acsestair.3c00098

Notes

The authors declare no competing financial interest.

ACKNOWLEDGMENTS

This work was supported by the NSF Center for Aerosol Impacts on Chemistry of the Environment under Grant CHE 1801971 and by NSF CHE 2304886. The authors would like to acknowledge the contributions of James Lazarcik at the University of Wisconsin-Madison Water Science and Engineering Laboratory for support with measuring sulfate samples by ion chromatography.

REFERENCES

- (1) Bates, T. S.; Lamb, B. K.; Guenther, A.; Dignon, J.; Stoiber, R. E. Sulfur emissions to the atmosphere from natural sources. *Journal of Atmospheric Chemistry* **1992**, *14* (1), 315–337.
- (2) Lana, A.; Bell, T. G.; Simó, R.; Vallina, S. M.; Ballabrera-Poy, J.; Kettle, A. J.; Dachs, J.; Bopp, L.; Saltzman, E. S.; Stefels, J.; et al. An updated climatology of surface dimethlysulfide concentrations and emission fluxes in the global ocean. *Global Biogeochemical Cycles* **2011**, 25 (1), GB1004.
- (3) Galí, M.; Levasseur, M.; Devred, E.; Simó, R.; Babin, M. Seasurface dimethylsulfide (DMS) concentration from satellite data at global and regional scales. *Biogeosciences* **2018**, *15* (11), 3497–3519.
- (4) Korhonen, H.; Carslaw, K. S.; Spracklen, D. V.; Mann, G. W.; Woodhouse, M. T. Influence of oceanic dimethyl sulfide emissions on cloud condensation nuclei concentrations and seasonality over the remote Southern Hemisphere oceans: A global model study. *Journal of Geophysical Research Atmospheres* **2008**, *113* (15), 1–16.
- (5) Vallina, S. M.; Simó, R.; Gassó, S. What controls CCN seasonality in the Southern Ocean? A statistical analysis based on satellite-derived chlorophyll and CCN and model-estimated OH radical and rainfall. *Global Biogeochemical Cycles* **2006**, *20* (1), 1–13.
- (6) von Glasow, R.; von Kuhlmann, R.; Lawrence, M. G.; Platt, U.; Crutzen, P. J. Impact of reactive bromine chemistry in the troposphere. *Atmos. Chem. Phys.* **2004**, *4* (11/12), 2481–2497.
- (7) Boucher, O.; Moulin, C.; Belviso, S.; Aumont, O.; Bopp, L.; Cosme, E.; Von Kuhlmann, R.; Lawrence, M. G.; Pham, M.; Reddy, M. S.; et al. DMS atmospheric concentrations and sulphate aerosol indirect radiative forcing: A sensitivity study to the DMS source representation and oxidation. *Atmospheric Chemistry and Physics* **2003**, 3 (1), 49–65.
- (8) Faloona, I. Sulfur processing in the marine atmospheric boundary layer: A review and critical assessment of modeling uncertainties. *Atmospheric Environment* **2009**, *43* (18), 2841–2854.
- (9) Fung, K. M.; Heald, C.; Kroll, J.; Wang, S.; Jo, D.; Gettelman, A.; Lu, Z.; Liu, X.; Zaveri, R.; Apel, E.; et al. Exploring DMS oxidation and implications for global aerosol radiative forcing. *Atmospheric Chemistry and Physics* **2022**, *22*, 1549.
- (10) Hodshire, A. L.; Campuzano-Jost, P.; Kodros, J. K.; Croft, B.; Nault, B. A.; Schroder, J. C.; Jimenez, J. L.; Pierce, J. R. The potential role of methanesulfonic acid (MSA) in aerosol formation and growth and the associated radiative forcings. *Atmospheric Chemistry and Physics* **2019**, *19* (5), 3137–3160.
- (11) Jernigan, C. M.; Cappa, C. D.; Bertram, T. H. Reactive Uptake of Hydroperoxymethyl Thioformate to Sodium Chloride and Sodium Iodide Aerosol Particles. *J. Phys. Chem. A* **2022**, *126*, 4476.
- (12) Veres, P. R.; Andrew Neuman, J.; Bertram, T. H.; Assaf, E.; Wolfe, G. M.; Williamson, C. J.; Weinzierl, B.; Tilmes, S.; Thompson, C. R.; Thames, A. B.; et al. Global airborne sampling reveals a previously unobserved dimethyl sulfide oxidation mechanism in the marine atmosphere. *Proc. Natl. Acad. Sci. U.S.A.* **2020**, *117* (9), 4505–4510.
- (13) Vermeuel, M. P.; Novak, G. A.; Jernigan, C. M.; Bertram, T. H. Diel Profile of Hydroperoxymethyl Thioformate: Evidence for Surface Deposition and Multiphase Chemistry. *Environ. Sci. Technol.* **2020**, *54* (19), 12521–12529.
- (14) Berndt, T.; Scholz, W.; Mentler, B.; Fischer, L.; Hoffmann, E. H.; Tilgner, A.; Hyttinen, N.; Prisle, N. L.; Hansel, A.; Herrmann, H. Fast Peroxy Radical Isomerization and OH Recycling in the Reaction of OH Radicals with Dimethyl Sulfide. *J. Phys. Chem. Lett.* **2019**, *10* (21), 6478–6483.

- (15) Jernigan, C. M.; Fite, C. H.; Vereecken, L.; Berkelhammer, M. B.; Rollins, A. W.; Rickly, P. S.; Novelli, A.; Taraborrelli, D.; Holmes, C. D.; Bertram, T. H. Efficient Production of Carbonyl Sulfide in the Low-NO x Oxidation of Dimethyl Sulfide. *Geophysical Research Letters* **2022**, 49 (3), e2021GL096838—e092021GL096838.
- (16) Novak, G. A.; Fite, C. H.; Holmes, C. D.; Veres, P. R.; Neuman, J. A.; Faloona, I.; Thornton, J. A.; Wolfe, G. M.; Vermeuel, M. P.; Jernigan, C. M.; et al. Rapid cloud removal of dimethyl sulfide oxidation products limits SO 2 and cloud condensation nuclei production in the marine atmosphere. *Proc. Natl. Acad. Sci. U. S. A.* **2021**, *118* (42), No. e2110472118.
- (17) Bertram, T. H.; Kimmel, J. R.; Crisp, T. A.; Ryder, O. S.; Yatavelli, R. L. N.; Thornton, J. A.; Cubison, M. J.; Gonin, M.; Worsnop, D. R. A field-deployable, chemical ionization time-of-flight mass spectrometer. *Atmospheric Measurement Techniques* **2011**, *4* (7), 1471–1479.
- (18) Novak, G.; Vermeuel, M.; Bertram, T. Simultaneous Detection of Ozone and Nitrogen Dioxide by Oxygen Anion Chemical Ionization Mass Spectrometry: A Fast Time Response Sensor Suitable for Eddy Covariance Measurements. *Atmos. Meas. Tech.* **2020**, *13*, 1887.
- (19) Huey, L. G. Measurement of trace atmospheric species by chemical ionization mass spectrometry: Speciation of reactive nitrogen and future directions. *Mass Spectrom. Rev.* **2007**, 26 (2), 166–184.
- (20) Berkelhammer, M.; Asaf, D.; Still, C.; Montzka, S.; Noone, D.; Gupta, M.; Provencal, R.; Chen, H.; Yakir, D. Constraining surface carbon fluxes using in situ measurements of carbonyl sulfide and carbon dioxide. *Global Biogeochemical Cycles* **2014**, 28 (2), 161–179.
- (21) Bunk, R.; Behrendt, T.; Yi, Z.; Andreae, M. O.; Kesselmeier, J. Exchange of carbonyl sulfide (OCS) between soils and atmosphere under various CO2 concentrations. *Journal of Geophysical Research: Biogeosciences* **2017**, *122* (6), 1343–1358.
- (22) Vaughan, S.; Canosa-Mas, C. E.; Pfrang, C.; Shallcross, D. E.; Watson, L.; Wayne, R. P. Kinetic studies of reactions of the nitrate radical (NO 3) with peroxy radicals (RO 2): an indirect source of OH at night? *Physical Chemistry Chemical Physics* **2006**, 8 (32), 3749–3760.
- (23) Burkholder, J.; Sander, S.; Abbatt, J.; Barker, J.; Cappa, C.; Crounse, J.; Dibble, T.; Huie, R.; Kolb, C.; Kurylo, M. Chemical kinetics and photochemical data for use in atmospheric studies; evaluation number 19; Jet Propulsion Laboratory, National Aeronautics and Space: Pasadena, CA, 2020.
- (24) Barnes, I.; Hjorth, J.; Mihalapoulos, N. Dimethyl sulfide and dimethyl sulfoxide and their oxidation in the atmosphere. *Chem. Rev.* **2006**, *106* (3), 940–975.
- (25) Schwarzenbach, R. P.; Gschwend, P. M.; Imboden, D. M. Environmental organic chemistry; John Wiley & Sons: 2016.
- (26) Lee, Y.-N.; Zhou, X. Aqueous reaction kinetics of ozone and dimethylsulfide and its atmospheric implications. *Journal of Geophysical Research: Atmospheres* **1994**, 99 (D2), 3597–3605.
- (27) Gershenzon, M.; Davidovits, P.; Jayne, J. T.; Kolb, C. E.; Worsnop, D. R. Simultaneous Uptake of DMS and Ozone on Water. *J. Phys. Chem. A* **2001**, *105* (29), 7031–7036.
- (28) Kercher, J. P.; Riedel, T. P.; Thornton, J. A. Chlorine activation by N_2O_5 : simultaneous, in situ detection of ClNO₂ and N_2O_5 by chemical ionization mass spectrometry. *Atmos. Meas. Technol.* **2009**, 2 (1), 193–204.
- (29) Lee, B. H.; Lopez-Hilfiker, F. D.; Mohr, C.; Kurtén, T.; Worsnop, D. R.; Thornton, J. A. An Iodide-Adduct High-Resolution Time-of-Flight Chemical-Ionization Mass Spectrometer: Application to Atmospheric Inorganic and Organic Compounds. *Environ. Sci. Technol.* **2014**, *48* (11), 6309–6317.
- (30) Robinson, M. A.; Neuman, J. A.; Huey, L. G.; Roberts, J. M.; Brown, S. S.; Veres, P. R. Temperature-dependent sensitivity of iodide chemical ionization mass spectrometers. *Atmos. Meas. Technol.* **2022**, *15* (14), 4295–4305.
- (31) Elliott, S.; Lu, E.; Rowland, F. S. Rates and Mechanisms for the Hydrolysis of Carbonyl Sulfide in Natural Waters. *Environ. Sci. Technol.* 1989, 23 (4), 458–461.
- (32) Dovrou, E.; Rivera-Rios, J. C.; Bates, K. H.; Keutsch, F. N. Sulfate Formation via Cloud Processing from Isoprene Hydroxyl Hydro-

- peroxides (ISOPOOH). Environ. Sci. Technol. 2019, 53 (21), 12476–12484.
- (33) Lind, J. A.; Lazrus, A. L.; Kok, G. L. Aqueous phase oxidation of sulfur (IV) by hydrogen peroxide, methylhydroperoxide, and peroxyacetic acid. *Journal of Geophysical Research: Atmospheres* **1987**, 92 (D4), 4171–4177.
- (34) Martin, L. R.; Damschen, D. E.; Judeikis, H. S. The reactions of nitrogen oxides with SO2 in aqueous aerosols. *Atmospheric Environment* (1967) 1981, 15 (2), 191–195.
- (35) Kroll, J. H.; Ng, N. L.; Murphy, S. M.; Varutbangkul, V.; Flagan, R. C.; Seinfeld, J. H. Chamber studies of secondary organic aerosol growth by reactive uptake of simple carbonyl compounds. *Journal of Geophysical Research Atmospheres* **2005**, *110* (23), 1–10.
- (36) Liggio, J.; Li, S. M. Reactive uptake of pinonaldehyde on acidic aerosols. *Journal of Geophysical Research Atmospheres* **2006**, 111 (24), 1–12.
- (37) Liggio, J.; Li, S. M.; McLaren, R. Reactive uptake of glyoxal by particulate matter. *Journal of Geophysical Research D: Atmospheres* **2005**, 110 (10), 1–13.
- (38) Moshammer, K.; Jasper, A. W.; Popolan-Vaida, D. M.; Lucassen, A.; Diévart, P.; Selim, H.; Eskola, A. J.; Taatjes, C. A.; Leone, S. R.; Sarathy, S. M.; et al. Detection and Identification of the Keto-Hydroperoxide (HOOCH2OCHO) and Other Intermediates during Low-Temperature Oxidation of Dimethyl Ether. *J. Phys. Chem. A* **2015**, 119 (28), 7361–7374.
- (39) Moshammer, K.; Jasper, A. W.; Popolan-Vaida, D. M.; Wang, Z.; Bhavani Shankar, V. S.; Ruwe, L.; Taatjes, C. A.; Dagaut, P.; Hansen, N. Quantification of the Keto-Hydroperoxide (HOOCH2OCHO) and Other Elusive Intermediates during Low-Temperature Oxidation of Dimethyl Ether. *J. Phys. Chem. A* **2016**, *120* (40), 7890–7901.
- (40) Neeb, P.; Horie, O.; Moortgat, G. K. The nature of the transitory product in the gas-phase ozonolysis of ethene. *Chemical Physics Letters* **1995**, 246 (1), 150–156.
- (41) Thamm, J.; Wolff, S.; Turner, W. V.; Gäb, S.; Thomas, W.; Zabel, F.; Fink, E. H.; Becker, K. H. Proof of the formation of hydroperoxymethyl formate in the ozonolysis of ethene: synthesis and FT-IR spectra of the authentic compound. *Chemical Physics Letters* **1996**, 258 (1), 155–158.
- (42) Pagonis, D.; Ziemann, P. J. Chemistry of hydroperoxycarbonyls in secondary organic aerosol. *Aerosol Science and Technology* **2018**, *52* (10), 1178–1193.
- (43) Gligorovski, S.; Strekowski, R.; Barbati, S.; Vione, D. Environmental Implications of Hydroxyl Radicals (•OH). *Chem. Rev.* **2015**, 115 (24), 13051–13092.
- (44) Jackson, A.; Hewitt, C. Atmosphere hydrogen peroxide and organic hydroperoxides: a review. *Critical Reviews in Environmental Science and Technology* **1999**, 29 (2), 175–228.
- (45) Fausto, R.; Carvalho, L. A. E. B. d.; José, J. C. T.-D. Molecular structure and properties of thioacetic acid. *Journal of Molecular Structure: THEOCHEM* **1990**, 207, 67–83.
- (46) Glavas, S.; Toby, S. Reaction between ozone and hydrogen sulfide. J. Phys. Chem. 1975, 79 (8), 779–782.
- (47) Mark, G.; Naumov, S.; von Sonntag, C. The Reaction of Ozone with Bisulfide (HS-) in Aqueous Solution Mechanistic Aspects. *Ozone: Science & Engineering* **2011**, 33 (1), 37–41.
- (48) Schmitz, L. R. Aqueous phase ozonation of methanethiol and dimethyl disulfide; 1973.
- (49) Barnard, D. 914. Oxidation of organic sulphides. Part IX. The reaction of ozone with organic sulphur compounds. *Journal of the Chemical Society (Resumed)* **1957**, 4547–4555.
- (50) Schiff, H. Eine neue Reihe organischer Diamine. *Justus Liebigs Annalen der Chemie* **1866**, 140 (1), 92–137.
- (51) Munger, J. W.; Jacob, D. J.; Hoffmann, M. R. The occurrence of bisulfite-aldehyde addition products in fog- and cloudwater. *Journal of Atmospheric Chemistry* **1984**, *1* (4), 335–350.
- (52) Boyce, S. D.; Hoffmann, M. R. Kinetics and mechanism of the formation of hydroxymethanesulfonic acid at low pH. *J. Phys. Chem.* **1984**, 88 (20), 4740–4746.